Applied Chemical Engineering (2020) Volume 3 Issue 2
doi:10.24294/ace.v3i2.714

ORIGINAL RESEARCH ARTICLE

Convective flow boiling heat transfer in an annular space: N-heptane/water case in a bubbly sub-cooled flow

M. M. Sarafraz[1*], H. Arya[2]

[1] *Faculty of Chemical, Petroleum and Gas Engineering, Semnan University, Semnan, Iran. E-mail: mohamadmohsensarafraz@gmail.com*

[2] *Center for Energy Resource Engineering, Technical University of Denmark, Denmark*

ABSTRACT

The subcooled flow boiling heat transfer characteristics of n-heptane and water is conducted for an upward flow inside the vertical annulus with an inner gap of 30 mm, in different heat fluxes up to 132kW.m^{-2}, subcooling max.:30C, flow rate: 1.5 to 3.5lit.min^{-1} under the atmospheric pressure. The measured data indicate that the subcooled flow boiling heat transfer coefficient significantly increases with increasing liquid flow rate and heat flux and slightly decreases with decreasing the subcooling level. Although results demonstrate that subcooling is the most effective operation parameter on onset of nucleate boiling such that with decreasing the subcooling level, the inception heat flux significantly decreases. Besides, recorded results from the visualization of flow show that the mean diameter of the bubbles departing from the heating surface decreases slightly with increasing the flow rate and slightly decreases with decreasing the subcooling level. Meanwhile, comparisons of the present heat transfer data for n-heptane and water in the same annulus and with some existing correlations are investigated. Results of comparisons reveal an excellent agreement between experimental data and those of calculated by Chen Type model and Gungor–Winterton predicting correlation.

***Keywords*:** Annular Flow; Nucleate Flow Boiling; Subcooled; Pure Liquid; Convective; Heat Transfer

ARTICLE INFO

Received 19 August 2020
Accepted 12 September 2020
Available online 16 September 2020

1. Introduction

Flow boiling has long played a major role in many technological applications due to its superior heat transfer performance. The complexities encountered in the boiling process have stimulated numerous investigators to conduct extensive research in this field. Because of unknown properties which are hidden inside of boiling phenomenon, many investigators have conducted large number of experiments on different substances. This complexity is due to the heterogeneous nature of heat transfer medium. Boiling of liquid mixtures is furthermore integrated with simultaneous heat and mass transfer between vapor inside the bubble and the vapor/liquid interface, which makes the phenomenon much more complicated. So far, the boiling phenomenon has not been modeled through any simple theoretical model. Flow boiling heat transfer is also one of the major interests to designers of water liquid cooled nuclear reactors. One source of concern is reactor behavior following a hypothetical loss-of-flow accident or cooling flow was unable to provide the sufficient heat transfer. In this particular case, exceeding the heat flux up to critical heat flux can lead to irrecoverable damages to the reactor and industrial installations. Subcooled boiling is characterized by the

generation of vapour bubbles at the heater surface, while the bulk temperature of the liquid is still below the saturation temperature. Bubbles detaching from the heat transfer surface collapse and condense in the subcooled liquid bulk, while this situation basically occurs in almost every reactor or high temperature surfaces. It is particularly significant in nuclear reactors and even around the rod fuel pools. Many researchers have been performed several experiments to investigate the effects of various parameters on the subcooled flow boiling heat transfer. On the basis of the coolant fluid component(s), conducted researches may be sorted in terms of investigation on the subcooled flow boiling heat transfer to either pure liquids or mixtures, although the main object of this experimental study is to investigate the first group of test fluids.

2. Literature review

As an example of conducted researches, Zeitoun[1] performed a subcooled boiling test in a high heat flux condition. However, the test section for the boiling heat transfer was short in length and local bubble parameters were not provided. Early visualization experiments carried out by Hewitt *et al*.[2] showed that the bubbles affect the nucleation activity. The presence of moving bubbles leads to the wave-induced nucleation phenomenon observed by Barbosa *et al*.[3]. He conducted experiments in a vertical annulus in which heat was applied to the inner surface of the tube. A dominance of nucleate boiling was observed at low qualities. At high qualities, nucleate boiling was partly or totally suppressed and forced convection became the dominant mechanism. Thus, one may conclude that in internal flow boiling, the heat transfer coefficient is a combination of two mechanisms: nucleate boiling and forced convection. The heat transfer coefficient might remain constant, decrease or increase depending on the contribution of these two mechanisms during forced saturation boiling. You *et al*.[4] conducted experiments on subcooled flow boiling heat transfer of water-sugar mixture to show the effects of heat flux, fluid velocity, and subcooling on the enhancement of nucleate boiling heat transfer in the partial flow boiling regime, where both forced convection and nucleate boiling heat transfer occurred. They found that increasing the sugar concentration led to a significant drop in the observed heat transfer coefficient because of a mixture effect, which resulted in a local rise in the saturation temperature of sugar solution at the vapor-liquid interface. Peyghambarzadeh *et al*.[5] performed a large number of experiments to measure the heat transfer reduction and fouling resistance of $CaSO_4$ aqueous solutions and pure water in a vertical upward annulus under subcooled flow boiling condition. Experiments are designed so that the effects of different parameters such as solution concentration, wall temperatures, and heat flux as well as flow velocity on flow boiling heat transfer coefficient would be clarified. Ahmady *et al*.[6] conducted the experimental study of onset of subcooled annular flow boiling and surveyed the effect of pressure, mass flux, and inlet temperature of annulus on the inception heat flux. They illustrated that inlet temperature directly influences on the inception heat flux. For an extensive literature survey of flow boiling in conventional-size channels, the interested readers are referred to Kew and Cornwell[7] and Lin *et al*.,[8] or for small-diameter channels to Kandlikar and Grande[9] and Kandlikar[10], or Chen[11] and Bergles *et al*.[12] In general, all existing approaches are either the empirical fits to the experimental data, or form an attempt to combine two major influences to heat transfer, namely, the convective flow boiling without bubble generation, and the nucleate boiling. Generally, that is done in a linear or nonlinear manner. Alternatively, there is a group of modern approaches based on models that start from modeling a specific flow structure and in such a way postulate more accurate flow boiling models, usually pertinent to slug and annular flows. One of the first major works in this area was that of Celata *et al*.[13] who reported data for binary mixtures in forced convection zone. They compared their data with other correlations such as Guerrieri and Talty[14], but in each case, found considerable scatter. They then proposed their own correlation. Chang

and Kim[15] presented a survey of performance and heat transfer characteristics of hydrocarbon refrigerants and their mixtures (R290, R600, R600a, R290/R600and R290/R600) in a heat pump system. Sivagnanam *et al*.[16] studied subcooled flow boiling of binary mixtures on a long platinum wire and proposed correlations for the partial boiling and fully developed boiling. Ose and Kunigu[17] conducted the experiments in order to clarify the heat transfer characteristics of the subcooled pool boiling and to discuss the effect of various parameters on the flow boiling heat transfer. A boiling and condensation model for numerical simulation of subcooled boiling phenomenon was developed too. Lima *et al*.[18] presented flow boiling heat transfer results of R-134a flowing inside a 13.84 mm internal diameter, smooth horizontal copper tube. They investigated the effect of types of flow on the flow boiling heat transfer mechanism and presented that a local minimum heat transfer coefficient systematically occurs within slug flow pattern or near the slug-to-intermittent flow pattern transition. The vapor quality at which the local minimum occurs seems to be primarily sensitive to mass velocity and heat flux. Thus, it is influenced by the competition between nucleate and convective boiling mechanisms that control the flow boiling. Hou *et al*.[19] investigated the boiling heat transfer in small diameter tubes using R134a as the working fluid. The heat transfer experiments were conducted with two stainless steel tubes of internal diameter 4.26 and 2.01 mm. They also conducted the flow visualization experiments using the same experimental facility with Pyrex glass tubes. A flow pattern map was obtained at a system pressure of 10 bar and tube diameter of 4.26 mm and the effects of different operating parameters on the flow boiling heat transfer coefficient have been experimentally investigated. Celata *et al*.[20] presented the results of the flow boiling patterns of FC-72 in a micro-tube inside the pyrex glass tube in order to obtain the visualization of the flow pattern along the heated channel. Different types of flow pattern were observed. The experiments represented various data at related heat fluxes and low sub-cooling levels. They showed different flow patterns in the presence of flow instabilities in bubbly/slug flow and slug/annular flow. Orian *et al*.[21] conducted experimental study on the flow boiling of binary organic solution in a horizontal tube. An organic mixture of miscible fluids, chlorodifluoromethane (R22)–dimethyl-la-cetamide (DMAC) was circulated through the experimental system. The influence of the heat source, flow rate, solution concentration, and operating pressure on the flow characteristics and the heat transfer coefficient was examined experimentally. Based on the experimental observation, an appropriate flow pattern map was constructed. Hetsroni *et al*.[22] studied the influence of concentration of surfactants on augmentation of heat transfer coefficient of mixtures inside the annulus and compared the results to that of pure water. They also reported that the addition of surfactant to the water produced a large number of bubbles of small diameter, which, at high heat fluxes, tend to cover the entire heater surface with a vapor blanket. Similarly, Inoue and Monde[23] investigated the effect of surfactant on the enhancement of the heat transfer coefficient in deionized water and ammonia/water mixtures. More relevant studies may also be found in the literature[24–27].

The objective of this study is to identify the effect of operation parameters on subcooled flow boiling and comparing the experimental data with existing correlations. Several experiments were conducted covering different ranges of flow rate, inlet temperature (subcooling effect) and heat flux inside the vertical annulus. On the contrary, to similar earlier works, moreover than investigating on the effect of these operation parameters on flow boiling heat transfer coefficient, influence of operation parameters on the visualized mean bubble diameter size have simultaneously been surveyed. Then after, comparisons between some well-known predicting correlations (Chen type model and Gungor-Winterton) and experimental data were comparatively performed. For these models, results reveal the fair agreement between experimental data and those of calculated by correlations.

3. Experimental

3.1. Experimental apparatus

Figure 1 shows the test apparatus used for the present investigation. The liquid flows in a closed loop consisting of temperature controlled storage tank, centrifugal pump and the annular test section. The flow velocity of the fluid was measured with a calibrated vertical rotameter (manufactured by Sarir-teb Co.). The fluid temperature was measured by two PT-100 thermometers installed in two thermo-well located just before and after the annular section. The complete cylinder was made from stainless steel 316a. Thermometer voltages, current and voltage drop from the test heater were all measured and processed with a data acquisition system in conjunction with a PID temperature controller. The test section shown in **Figure 2** consists of an electrically heated cylindrical DC bolt heater (manufactured by Cetal Co.) with a stainless steel surface, which is mounted concentrically within the surrounding pipe. The dimensions of the test section are: diameter of heating rod, 20 mm; annular gap diameter (hydraulic diameter), 30 mm; the length of the pyrex tube, 500 mm; the length of stainless steel rod, 350 mm; the length of heated section, 150 mm which means that just the first 150 mm of stainless steel is heated uniformly and radially by the heater. The axial heat transfer thorough the rod can be ignored according to the insulation of the both ends of the heater. The heat flux and wall temperature can be as high as 132,000 $W.m^{-2}$ and 150°C, respectively. The local wall temperatures have been measured with four stainless steel sheathed K-type thermocouples which have been installed close to the heat transfer surface. The temperature drop between the thermocouples location and the heat transfer surface can be calculated from:

$$T_w = T_{th} - \dot{q}\frac{s}{\lambda_w} \quad (1)$$

The ratio between the distance of the thermometers from the surface and the thermal conductivity of the tube material (s/λ_w) was determined for each K-type thermocouple by calibration using Wilson plot technique[28]. The average temperature difference for each test section was the arithmetic average of the four thermometers readings around the rod circumference. The average of 10 voltage readings was used to determine the difference between the wall and bulk temperature for each thermometer. All the K-type thermocouples were thoroughly calibrated using a constant temperature water bath, and their accuracy has been estimated to ±0.3K. The local heat transfer coefficient α is then calculated from:

$$\alpha = \frac{\dot{q}}{(T_w - T_b)_{ave.}} \quad (2)$$

To minimize the thermal contact resistance, high quality silicone paste was injected into the thermocouple wells. To avoid possible heat loss, main tank circumferences were heavily insulated using industrial glass wool. To control the fluctuations due to the alternative current, a regular DC power supply was also employed to supply the needed voltage to central heater. Likewise, to visualize the flow and boiling phenomenon and record the proper images, annulus was made of the pyrex glass. More details of the test section and apparatus are given in **Figures (1-2)**.

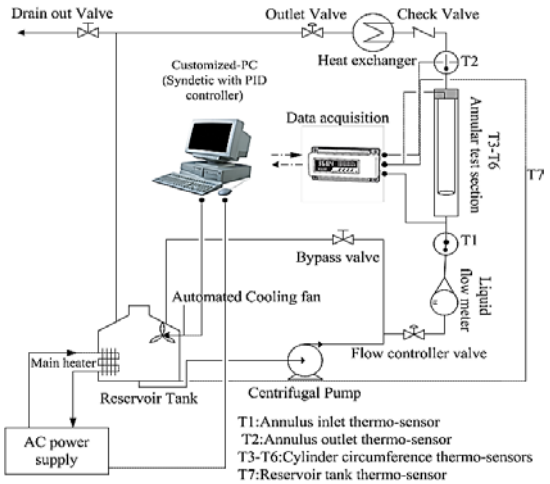

Figure 1. A scheme of the experimental apparatus.

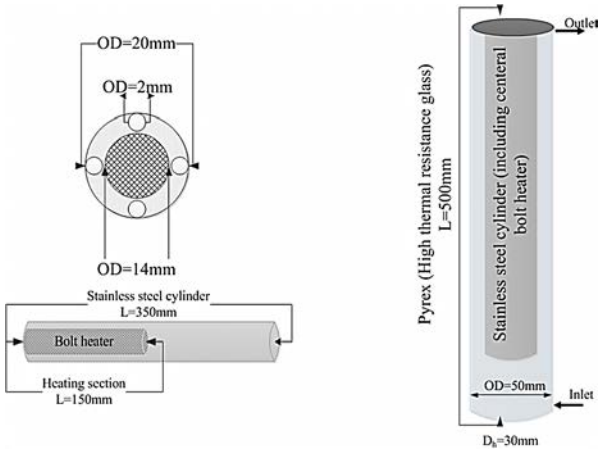

Figure 2. Details of the annular space and the heating section.

3.2 Experiment procedure

Prior to commencing a test run, test heater, reservoir tanks and pipes were acid washed and were cleaned to remove any scale from previous experiments. Once the system was cleaned, the test solution and the cleaning agent were introduced to the reservoir tanks. Following this, the tank heater was switched on and the temperature of the system increased. When the fluid had reached the desired temperature, the pump was started and the rig allowed to be stabilized at the desired bulk temperature and velocity. Then, the power was supplied to the test heater and kept at a pre-determined value. The data acquisition system was switched on and temperatures, pressure and heat flux were recorded.

3.3 Error analysis

The uncertainties of the experimental results are analyzed by the procedures proposed by Kline and McClintock[29]. The method is based on careful specifications of the uncertainties in the various primary experimental measurements. The heat transfer coefficient can be obtained using Eq. (3):

$$\alpha = \frac{\rho V Cp(T_{out} - T_{in})}{(T_w - T_b)_{av.}} \quad (3)$$

As seen from Eq. (3), the uncertainty in the measurement of the heat transfer coefficient can be related to the errors in the measurements of volume flow rate, hydraulic diameter, and all the temperatures as follows.

$$\alpha = f\ \{V, A_h, (T_{out} - T_{in}), (T_w - T_b)\} \quad (4)$$

$$\partial\alpha = \sqrt{\left[\left(\frac{\partial\alpha}{\partial V}\right).\delta V\right]^2 + \left[\left(\frac{\partial\alpha}{\partial A}\right).\delta A\right]^2 + \left[\left(\frac{\partial\alpha}{\partial(Tout - Tin)}\right).\delta(Tout - Tin)\right]^2 + \left[\left(\frac{\partial\alpha}{\partial(Tw - Tb)}\right).\delta(Tw - Tb)\right]^2} \quad (5)$$

According to the above uncertainty analysis, the uncertainty in the measurement of the heat transfer coefficient is 16.23%. The detailed results from the present uncertainty analysis for the experiments conducted here are summarized in **Table 1**. The main source of uncertainty is due to the temperature measurement and its related devices.

Table 1. Summary of the uncertainty analysis

Parameter	Uncertainty
Length, width and thickness, (m)	± 0.0005
Temperature, (K)	± 0.3*K*
Water flow rate, (lit. min^{-1})	± 1.5% of readings
Voltage, (V)	± 1% of readings
Current, (A)	± 0.02% of readings
Cylinder side area, (m^2)	± 4×10^{-8}
Flow boiling heat transfer coefficient, ($W/m^2.K$)	± 16.23%

3.4 Operation parameters

The experimental apparatus provides the particular conditions to investigate the influence of heat fluxes, flow velocity, subcooling, and even concentration of mixture on flow boiling heat transfer coefficient (if binary or multi-component mixture is existed). Many experiments have been performed to investigate the effects of the operation parameters and subsequently, different values of parameters have been recorded. **Table 2** expresses the operation parameter conditions for water and n-heptane test fluids.

Table 2. Operation parameter values and experimental data

Parameter	Heat flux	Flow rate	Subcooling
Unit (SI)	kW/m^2	Lit/min	°C
range	5-132	1.5-3.5	10-30
Pressure	**Reynolds number**	**Data points**	**Heat transfer coefficient**
kPa	[ ]	[ ]	W/m^2. K
101.325	1970-3890	176	1052-7023

3.5 Physical properties of tested mixture

Water and n-heptane has been used as the test solution. The reported numerical values of physical properties are found to be inconsistent from different sources. In this investigation, all the physical properties have been calculated using standard correlations with known values of maximum expected uncertainty. The critical constants have been calculated using Joback method[30]. Expected uncertainty is reported equal to 7 K (~1%) for Tc; 2 bar (~5%). Liquid density for mixtures has been calculated by Spencer and Danner[31] method with the maximum expected uncertainty of 7%. Liquid thermal conductivities for liquids had been predicted by methods summarized by Bruce *et al.*[32]. The expected uncertainties are reported less than 10% for pure

liquids and up to 8% for liquid mixtures. Heat capacities for liquids have been calculated using Ruziicka and Domalski[33] method, with the expected uncertainty less than 4%. The heat capacities of liquid mixtures are estimated by mole fraction averages of the pure component values.

3.6 Calibrating the test heater

For the calibration of the test heater the well-known Wilson plot[34] was used which is explained here briefly. **Figure 3** shows a simple demonstration of the test heater and the locations of the thermocouples in it.

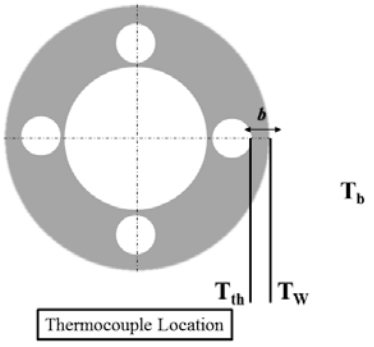

Figure 3. Thermocouple locations and calibration parameters**.**

As shown in **Figure 3**, the temperature shown by the thermocouple (T_{th}) is not exactly equal but it is slightly higher than the actual temperature of the heat transfer surface (T_w). This temperature difference is because of the conduction resistance of the heater material which is mounted between these two points. These temperatures can be related according to the energy balance under steady state condition:

$$\mathbf{q = U(T_{th} - T_b) = \alpha(T_w - T_b) = \frac{\lambda}{s}(T_{th} - T_w)} \quad (6)$$

This relation can be simplified as follows:

$$\frac{\mathbf{1}}{\mathbf{U}} = \frac{\mathbf{1}}{\boldsymbol{\alpha}} + \frac{\mathbf{s}}{\boldsymbol{\lambda}} \quad (7)$$

If α can be calculated using some characteristics of the system like velocity, estimation would be obtained for s/λusing Eq. (4). For this purpose, the below relation is used:

$$\boldsymbol{\alpha} \propto \mathbf{f.N_{Re}} \quad (8)$$

For the plain tubes, friction factor is related to Reynolds number according to Blasius relation as follows:

$$\mathbf{f} \propto \frac{\mathbf{1}}{\mathbf{N_{Re}^{0.25}}} \quad (9)$$

Having combinedtheequations 8 and 9, the following relation for heat transfer coefficient is obtained:

$$\boldsymbol{\alpha} \propto \mathbf{N_{Re}^{0.75}} \quad (10)$$

Since the bulk temperature is constant in each experiment, Reynolds number is proportional to the fluid velocity. Considering this point and unifying all the constants as "β", the following equation will be obtained:

$$\frac{\mathbf{1}}{\mathbf{U}} = \frac{\boldsymbol{\beta}}{\mathbf{V^{0.75}}} + \frac{\mathbf{s}}{\boldsymbol{\lambda}} \quad (11)$$

Eq. (11) shows that the plot of 1/U versus $1/V^{0.75}$ for each thermocouple gives the values of s/λ as the intercept of the line. **Figure 4** shows the calibration plot of the different thermocouples used in the test heater[35].

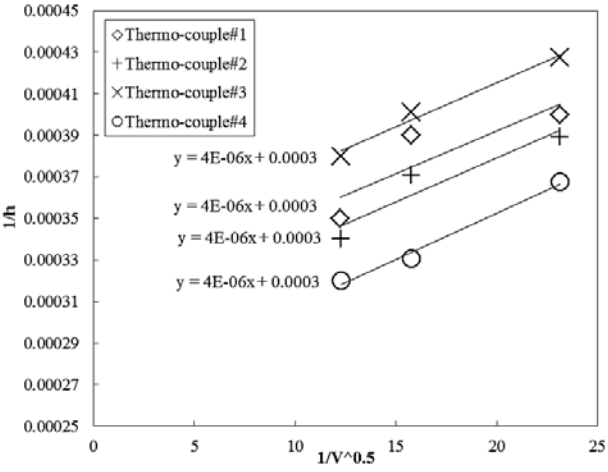

Figure 4. Calibration results for used K-type thermocouples**.**

This data were also taken under forced convective heat transfer to water at constant heat flux 8kW/m^2. As demonstrated in **Figure 4**, the values of s/λ for the thermocouples #1-4 are respectively equal to: 2.97×10^{-4}, 2.96×10^{-4}, 2.85×10^{-4}, 3.09×10^{-4} $m^2K.W^{-1}$. Performing the experiments again at other heat fluxes gives the value of $3\times10^{-4}m^2K.W^{-1}$as an average value of s/λ for all the thermocouples. This value was then used for the calibration of the surface thermocouples using Eq. (6).

4. Results and discussions

When we published our previous work[35], we

paid less attention to the effect of operating parameters on the generated bubbled diameters. Therefore, we were determined to investigate the effect of operating parameter on heat transfer coefficient, the bubble formation and size of mean bubble diameter separately.

4.1. Effect of heat flux

4.1.1 Effect of heat flux on flow boiling heat transfer coefficient

It is more convenient to show the effect of heat fluxon the flow boiling heat transfer coefficient in explicit terms of heat flux versus flow boiling heat transfer coefficient. **Figures (5-6)** show typical measured flow boiling heattransfer coefficients as a function of heat flux for pure n-heptane and deionized water, respectively, over a wide range of fluid velocity. Two distinct regimes can be observed: 1) at low heat fluxes, heat transfer occurs by convection mechanism and the heat transfer coefficient is almost independent of the heat flux and slightly changes can be observed with increasing the heat flux. It is because of the superimposed natural convection currents and due to changes in the physical properties of the fluids such as density, heat capacity and even viscosity of fluid, all as a result of the increased wall superheat. It must be Considered that natural convection is a result of density differences and is, therefore, most prominent at higher heat fluxes and low velocities.

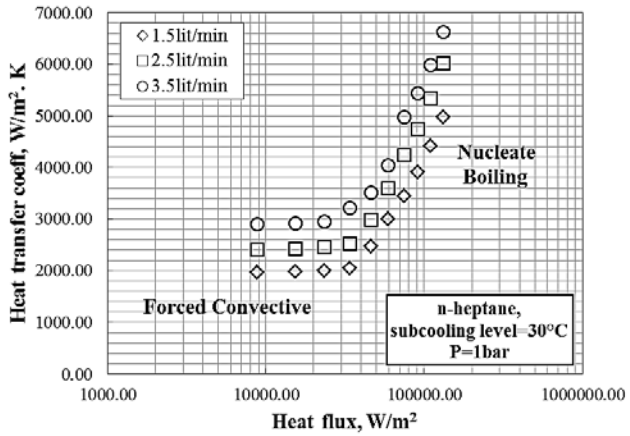

Figure 5. Forced convective and flow boiling heat transfer coefficient of n-heptane**.**

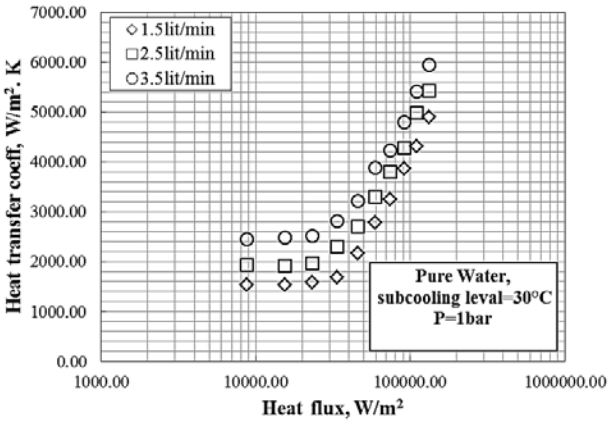

Figure 6. Forced convective and flow boiling heat transfer coefficient of water**.**

4.1.2 Effect of heat flux on visual bubble size

Many experiments have been performed to investigate the effect of heat flux on the bubble diameter. Visual recorded imagesdemonstrated that with increasing the heat flux (particularly at higher heat fluxes); the departure bubble diameter significantly increases over the different flow rates. In result of local vaporization inside the flow, amount of vapor that is captured inside the generated bubbles dramatically increases and subsequently, apparent size of bubbles increases. **Figures 7 (A-F)** depict the effect of heat flux on rate of bubble formation as well as the bubble diameter for n-heptane at different heat fluxes.

A **B**

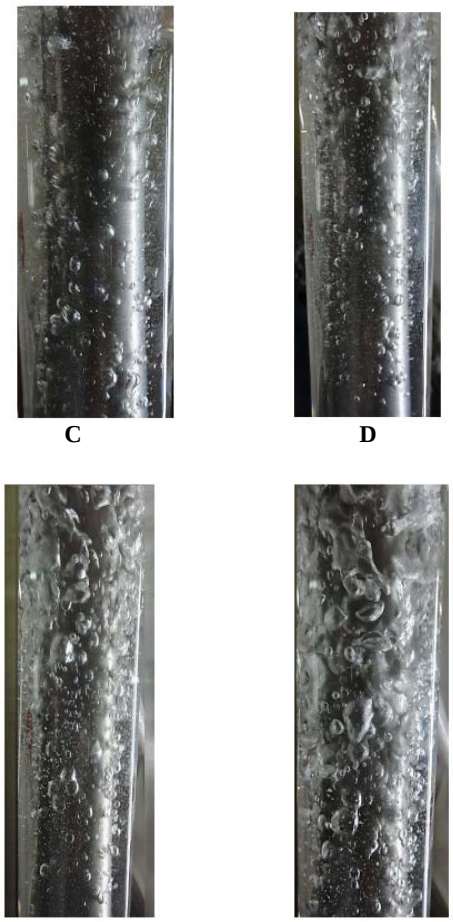

Figure 7. A: bubble formation at heat flux 45 kW/m^2; **B:** bubble formation at heat flux 54 kW/m^2; **C:** bubble formation at heat flux 63 kW/m^2; **D:** bubble formation at heat flux 91 kW/m^2; **E:** bubble formation at heat flux 110 kW/m^2; **F:** bubble formation at heat flux 132 kW/m^2**.**

4.2 Effect of fluid flow rate

4.2.1 Effect of liquid flow rate on heat transfer coefficient

Liquid flow rate may be considered as a one of the most effective parameter on flow boiling heat transfer coefficient so that with increasing the flow rate of fluid, the flow boiling heat transfer coefficient dramatically increases for both of n-heptane and pure water at any conditions, although flow rate has insignificant influence on the Forced convective heat transfer but in contrast, significant effect of flow rate is clearly seen on the flow boiling heat transfer mechanism and subsequently flow boiling heat transfer coefficient. **Figure 8** indicates the influence of flow rate on the Forced convective and flow boiling heat transfer coefficient for n-heptane. As can be seen, the higher flow rate, the higher flow boiling heat transfer coefficient is seen. Similar to n-heptane, for pure water the same condition can be seen and with increase of flow rate, higher flow boiling heat transfer coefficient is observed.

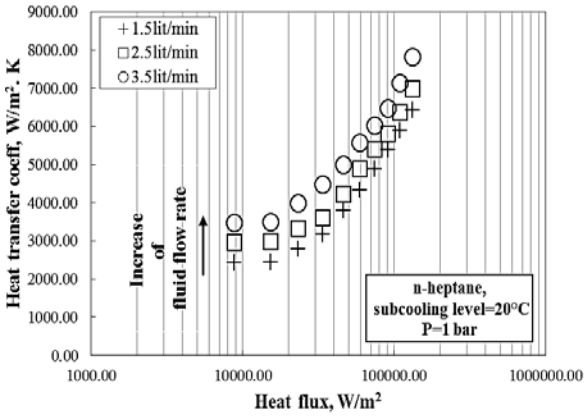

Figure 8. Effect of flow rate on flow boiling heat transfer coefficient of n-heptane (fordeionized water, similar condition is seen)**.**

4.2.2 Effect of fluid flow rate on bubble diameter

As can be seen in **Figure 9**, at lower flow rate, larger bubbles are observed at constant heat fluxes. It maybe occur due to the fact that the time needed for the growth of bubbles reduces at higher flow rates; therefore, bubbles are smaller than those observed at higher flow rates. Also, it is found that bubble diameter in water is smaller than that of n-heptane and frequency of bubble generation in water is greater than that of n-heptane. This point may lead to the postulation of lower boiling point for water than n-heptane which leads to more water turns to the vapor in comparison with n-heptane at particular, constant temperature.

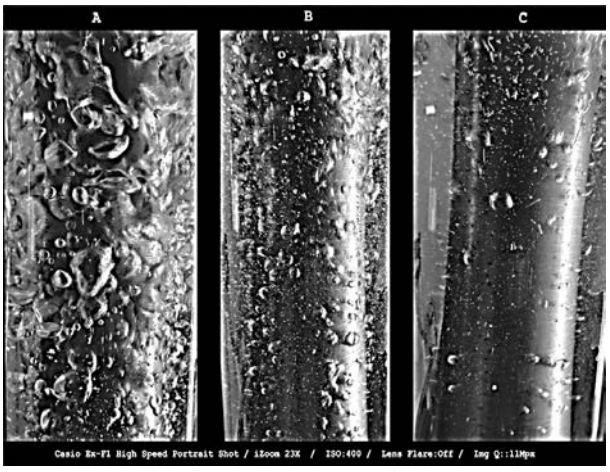

Figure 9. Effect of fluid flow rate on the bubble diameter in flow boiling of n-heptane at heat flux 85kW.m^{-2}: A: Q=1.5lit/min, B: Q=2.5lit/min, C: Q=3.5lit/min**.**

4.3 Effect of subcooling level (inlet temperature)

4.3.1 Effect of subcooling level on the flow boiling heat transfer coefficient

Figure 10 demonstrates the effect of liquid subcooling on the heat transfer coefficients of water and n-heptane at constant flow rate. Results show that the subcooled flow boiling heat transfer coefficient of both fluids increases as the subcooling increases. This increase in heat transfer coefficient manifests itself especially at higher heat fluxes. Conversely, under forced convective heat transfer regime, the subcooling temperature does not have strong influences on the heat transfer coefficient[35].

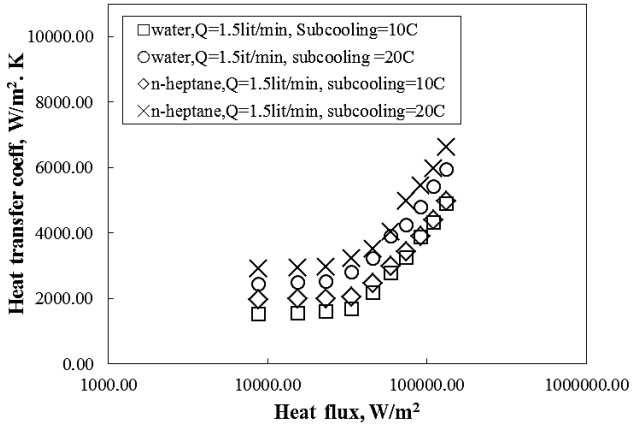

Figure 10. Comparison between heat transfer coefficient of flow boiling of n-heptane and water**.**

4.3.3 Effect of subcooling level on the bubble diameter

Many experiments were performed to find any correlation or rational relation between bubble diameter and subcooling level but they did not show any particular relationship between subcooling level and size of bubbles, however, more studies indicated that the only effect of subcooling level may be seen on the onset of nucleate boiling (ONB) where the first bubble arises from the heating section. In fact, the boundary between forced convective and nucleate boiling zone is ONB. Experiments show that the higher subcooling level causes that ONB point moved forward toward the higher heat flux, which means that at higher heat flux the first bubble is formed and seen. Briefly speaking, the lower subcooling level, the lower inception heat flux may be seen. **Figure 11** shows the effect of subcooling level on inception heat flux and ONB for both water and n-heptane test fluids.

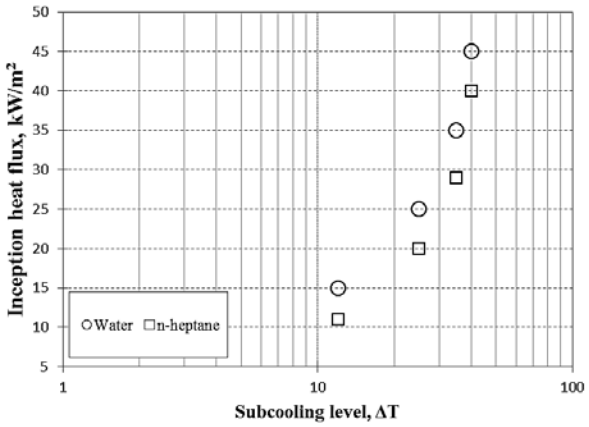

Figure 11. Influence of subcooling level on bubble characteristics**.**

4.4 Comparison of results with existing correlations

The obtained results may be used for engineering purposes[37-49]; therefore, these results must be compared with some well-known correlation to see how accurately these results are experimentally measured. The Chen model and Gungor-Winterton correlation are the ones of the most common used correlations used for predicting the flow boiling heat transfer coefficient. These correlations are given in **Table 3**.

No.	Author	Correlation
1	Chen(1966)	$\alpha_{fb} = S.\alpha_{nb} + F.\alpha_{fc}$ $F = \begin{cases} 1 & \text{if } \frac{1}{X_{tt}} \le 0.1 \\ 2.35\left(\frac{1}{X_{tt}} + 0.213\right)^{0.736} & \text{if } \frac{1}{X_{tt}} \ge 0.1 \end{cases}$ $S = \frac{1}{1 + 2.53?\ 0^{-6} N_{Re_{tp}}^{1.17}}$ $X_{tt} = \left(\frac{1-\dot{x}}{\dot{x}}\right)^{0.9}\left(\frac{\rho_v}{\rho_l}\right)^{0.5}\left(\frac{\mu_l}{\mu_v}\right)^{0.1}$ $\dot{x} = N_{Ph} - N_{Ph_n}\exp\left(\frac{N_{Ph}}{N_{Ph_n}} - 1\right)$ $N_{Ph} = \frac{h_v - h_{l,sat}}{h_{fg}}$ $N_{Ph_n} = \frac{-N_{Bo}}{\sqrt{\left(\frac{455}{N_{Pe_l}}\right)^2 + 0.0065^2}}$
2	Gungor and Winterton(1986)	$\alpha_{fb} = S.\alpha_{nb} + F.\alpha_{fc}$ $F = 1 + 24000 N_{BO}^{1.16} + 1.23\left(\frac{1}{x_{tt}}\right)^{0.86}$ $\alpha_{nb} = 55 P_r^{0.55}(-\log P_r)^{-0.55} M^{-0.5} q^{0.67}$
		The forced convective coefficient is calculated byDittus-Boelter

Figures (12-13) demonstrate the predicted results of flow boiling heat transfer coefficient of water and n-heptane using the Chen type model and Gungor-Winterton correlation. As can be seen, similar to our earlier work[38], results of Chen model are more reasonable when compared to Gungor-Winterton correlation. Besides, a deep look inside the both of figures demonstrates that for higher heat fluxes, both of correlations are unable to represent the good agreement between experimental results and those of obtained by the correlations. As seen, for Chen type model the Absolute Average Deviation of 20% is reported while it is about 30% for Gungor-Winterton correlation. Noticeably, Absolute Average Deviation is calculated using Eq. (12):

$$AAD\% = \frac{\alpha_{calculated} - \alpha_{experimental}}{\alpha_{experimental}} \times 100 \qquad (12)$$

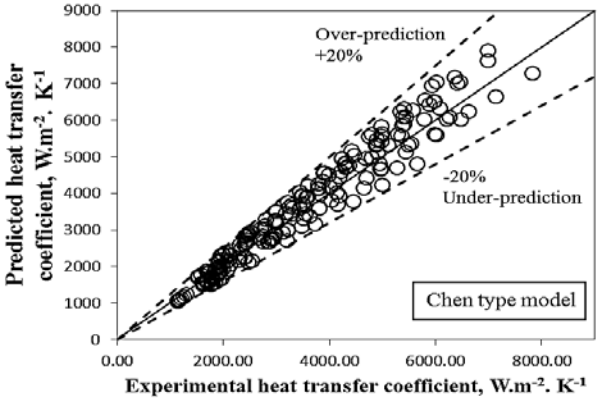

Figure 12. Results of comparison between experimental data and Chen type model.

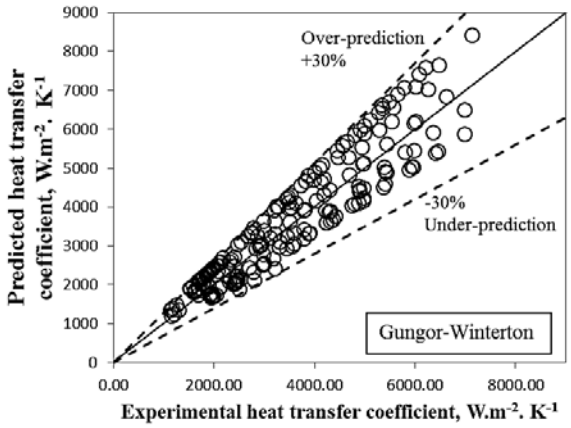

Figure 13. Results of comparison between experimental data and Gungor-Winterton correlation**.**

5. Conclusions

Experimental studies on flow boiling heat transfer coefficient of n-heptane and deionized-water were conducted. n-heptane after experiments is a plausible coolant almost identical to water. Investigations on the operating parameters showed that:

- Heat flux has an indispensible effect on the forced convective and nucleate flow boiling heat transfer regions such that with increasing the heat flux, heat transfer coefficient slightly, dramatically increases for forced convective, nucleate boiling regions respectively. Also with increasing the heat flux, rate of generated bubbles considerably increases.
- Flow rate of flow is also the other important operating parameters that with increasing the flow rate, heat transfer coefficient for forced convective and nucleate boiling regions dramatically increases. Also with increasing the flow rate, smaller bubbles are seen due to reduction of resident time of bubbles near the heating surface. Also increase of flow rate creates a chaotic flow which lead to bubbles to be collapsed near the surface and improve the convection currents which consequently enhances the heat transfer coefficient in nucleate boiling region.
- A rough comparison between results and available correlations showed that Chen type model predicts the experimental data with reasonable deviation of 20% which is 30% for Gungor-Winterton correlation.

Nomenclatures

A area, m^2
b distance, m
Bo boiling number
C_p heat capacity, $J.kg^{-1}.{}^oC^{-1}$
d_b bubble departing diameter, m
d_h hydraulic diameter, m
f fanning friction number
F enhancement factor
h enthalpy, $J.kg^{-1}$
ΔH_v heat of vaporization, $J.kg^{-1}$
k thermal conductivity, $W.m^{-1}.{}^oC^{-1}$
l_{th} heated length, m
L heater length, m
ΔL characteristic length in Eq. (15), m
Nu Nusselt number
Pe Peclet number
Ph phase change number
Pr reduced pressure
Pr Prandtl number
P pressure, Pa
q heat, W
Re Reynolds number
R_a roughness, m
s distance between thermometer location and heat transfer surface, m
S suppression factor
T temperature, K
x liquid mass or mole fraction
$\dot{x}$ vapour mass fraction
X_{tt} Martinelli parameter
y vapor mass or mole fraction

Subscripts-Superscripts

b bulk
c critical
fb flow boiling
in inlet
out outlet
l liquid
m mixture
n number of components
nb nucleate boiling
r reduced
Sat saturated
th thermometers
v vapor
w Wall

Greek symbols

α heat transfer coefficient, $W.m^{-2}.K^{-1}$

ρ density, $kg.m^{-3}$

μ viscosity, $kg.m^{-1}.s^{-1}$

Conflict of interest

The authors declare that they have no conflict of interest.

References

1. Zeitoun O. Subcooled flow boiling and condensation (Ph.D. Thesis). Canada: McMaster University; 1994.
2. Hewitt GF, Kersey HA, Lacey PMC, *et al*. Burnout and nucleation in climbing film flow. International Journal of Heat and Mass Transfer 1965; 8: 793–814.
3. Barbosa JR, Hewitt GF, Richardson SM. High-speed visualization of nucleate boiling in vertical annular flow. International Journal of Heat and Mass Transfer 2003; 46: 5153–5160.
4. You H, Sheikholeslami R, Doherty WOS. Flow boiling heat transfer of water and sugar solutions in an Annulus. Wiley Inter Science 2004; 50(6): 1119-1128.
5. Peyghambarzadeh SM, Vatani A, Jamialahmadi M. Application of asymptotic model for the prediction of fouling rate of calcium sulfate under sub-cooled flow boiling. Applied Thermal Engineering 2012; 39: 105-113.
6. Ahmadi R, Nouri-Borujerdi A, Jafari J, *et al*. Experimental study of onset of subcooled annular flow boiling. Progress in Nuclear Energy 2009; 51: 361–365.
7. Kew PA, Cornwell K. Correlations for the prediction of boiling heat transfer in small-diameter channels. Applied Thermal Engineering 1997; 17: 705–715.
8. Lin S, Kew PA, Cornwell K. Two-phase heat transfer to a refrigerant in a 1 mm diameter tube. International Journal of Refrigeration 2001; 24(1): 51–56.
9. Kandlikar SG, Grande WJ. Evolution of micro channel flow passages–Thermo hydraulic performance and fabrication technology. Heat Transfer Engineering 2003; 24(1): 3–17.
10. Kandlikar SG. Boiling heat transfer with binary mixtures; low boiling in plain tubes. Journal of Heat Transfer 1998; 120: 388–394.
11. Chen JC. A correlation for boiling heat transfer to saturated fluids inconvective flow. Industrial & Engineering Chemistry Process Design and Development 1966; 5(3): 322-329.
12. Bergles AE, Lienhard VJH, Kendall GE, *et al*. Boiling and evaporation in small diameter channels. Heat Transfer Engineering 2003; 24: 18–40.
13. Celata GP, Cumo M, Setaro T. Forced convective boiling in binary mixtures. International Journal of Heat and Mass Transfer 1993; 36(13): 3299–3309.
14. Guerrieri SA, Talty RD. Proposed correlation of data for two-phasecomponent flow in pipes. Chemical Engineering Progress Symposium Series 1956; 52: 69–77.
15. Chang YS, Kim MS. Performance and heat transfer characteristics of hydrocarbon refrigerants in a heat pump system. International Journal of Refrigeration 2000; 23: 232–242.
16. Sivagnanam P, Balakrishnan AR, Varma YBG. On the mechanism of subcooled flow boiling of binary mixtures. International Journal of Heat and Mass Transfer 1994; 37: 681–689.
17. Ose Y, Kunugi T. Development of a boiling and condensation model on subcooled boiling phenomena. Energy Procedia 2011; 9: 605–618.
18. Lima RJ, Quibén JM, Thome JR. Flow boiling in horizontal smooth tubes: New heat transfer results for R-134a at three saturation temperatures. Applied Thermal Engineering 2009; 29: 1289–1298.
19. Huo X, Chen L, Tian YS, *et al*. Flow boiling and flow regimes in small diameter tubes. Applied Thermal Engineering 2004; 24: 1225–1239.
20. Salari E, Peyghambarzadeh SM, Sarafraz MM, *et al*. Boiling thermal performance of TiO_2 aqueous nanofluids as a coolant on a disc copper block, Periodica Polytechnica. Chemical Engineering 2016; 60(2): 106.
21. Sarafraz MM. Nucleate pool boiling of aqueous solution of citric acid on a smoothed horizontal cylinder. Heat and Mass Transfer 2012; 48(4): 611–619.
22. Nakhjavani M, Nikkhah V, Sarafraz MM, *et al*. Green synthesis of silver nanoparticles using green tea leaves: Experimental study on the morphological, rheological and antibacterial behavior. Heat and Mass Transfer 2017; 53(10): 3201–3209.
23. Sarafraz M, Peyghambarzadeh S, Alavi Fazel S, *et al*. Nucleate pool boiling heat transfer of binary nano mixtures under atmospheric pressure around a smooth horizontal cylinder. Periodica Polytechnica: Chemical Engineering

2013; 57(1-2):71–77
24. Pourmehran O, Gorji TB, Gorji-Bandpy M, *et al*. Magnetic drug targeting through a realistic model of human tracheobronchial airways using computational fluid and particle dynamics. Biomechanics and Modeling in Mechanobiology 2016; 15(5): 1355–1374.
25. Zou X, Gong MQ, Chen GF, *et al*. Experimental study on saturated flow boiling heat transfer of R170/R290 mixtures in a horizontal tube. International Journal of Refrigeration 2010; 33: 371–380.
26. Lin PH, Fu BR, Chin Pan. Critical heat flux on flow boiling of methanol-water mixtures in a diverging micro-channel with artificial cavities. International Journal of Heat and Mass Transfer 2011; 54: 3156–3166.
27. Táboas F, Vallčs M, Bourouis M, *et al*. Assessment of boiling heat transfer and pressure drop correlations of ammonia/water mixture in a plate heat exchanger. International Journal of Refrigeration 2012; 35: 633–644.
28. Fernandez Seara J, Uhia FJ, Sieres J. Laboratory practices with the Wilson plot method. Experimental Heat Transfer 2007; 20: 123-135.
29. Kline SJ, McClintock FA. Describing uncertainties in single-sample experiments. Mechanical Engineering 1953; 75 (1): 3–12.
30. Joback KG. A unified approach to physical property estimation using multivariate statistical techniques (M.S. Thesis). Cambridge: Massachusetts Institute of Technology; 1984.
31. Spencer CF, Danner RP. Improved equation for prediction of saturated liquid density. Journal of Chemical & Engineering Data 1972; 17(2): 236–241.
32. Bruce E, Poling J, Prausnitz M, *et al*. The properties of gases and liquids, 5th ed. New York: The McGraw-Hill Companies; 2004. p. 10-11, 10-70.
33. Ruzicka V, Domalski ES. Estimation of the heat capacities of organic liquids as a function of temperature using group additives. Compounds of carbon, hydrogen, halogens, nitrogen, oxygen, and sulfur. Journal of Physical and Chemical Reference Data 1993; 22: 619–657.
34. Fernández-Seara J, Uhía FJ, Sieres J. Laboratory practices with the Wilsonplot method. Experimental Heat Transfer 2007; 20: 123–135.
35. Peyghambarzadeh SM, Sarafraz MM, Vaeli N, *et al*. Forced convective and subcooled flow boiling heat transfer to pure water and n-heptane in an annular heat exchanger. Annals of Nuclear Energy 2013; 53: 401–410.
36. Sarafraz MM, Peyghambarzadeh SM, Vaeli N. Subcooled flow boiling heat transfer of ethanol aqueous solutions in vertical annulus space. Chemical Industry & Chemical Engineering Quarterly 2012; 18(2): 315−327.
37. Sarafraz MM, Peyghambarzadeh SM. Experimental study on subcooled flow boiling heat transfer to water–diethylene glycol mixtures as a coolant inside a vertical annulus. Experimental Thermal and Fluid Science 2013; 50: 154–162.
38. Sarafraz MM, Peyghambarzadeh SM. Influence of thermodynamic models on the prediction of pool boiling heat transfer coefficient of dilute binary mixtures. International Communications in Heat and Mass Transfer 2012; 39(8): 1303–1310.
39. Biglarian M, Gorji MR, Pourmehran O, *et al*. H_2O based different nanofluids with unsteady condition and an external magnetic field on permeable channel heat transfer. International Journal of Hydrogen Energy 2017; 42 (34): 22005–22014.
40. Tabassum R, Mehmood R, Pourmehran O, *et al*. Impact of viscosity variation on oblique flow of Cu–H_2O nanofluid. Proceedings of the Institution of Mechanical Engineers, Part E: Journal of Process Mechanical Engineering 2017; 232(5): 622–631.
41. Sarafraz MM, Peyghambarzadeh SM, Nucleate pool boiling heat transfer to Al_2O_3-water and TiO2-water nanofluids on horizontal smooth tubes with dissimilar homogeneous materials. Chemical and Biochemical Engineering Quarterly 2012; 26 (3): 199-206.
42. Sarafraz MM, Peyghambarzadeh SM, Alavifazel SA. Enhancement of nucleate pool boiling heat transfer to dilute binary mixtures using endothermic chemical reactions around the smoothed horizontal cylinder. Heat and Mass Transfer 2012; 48 (10): 1755–1765.
43. Sarafraz MM, Hormozi F. Forced convective and nucleate flow boiling heat transfer to alumnia nanofluids. Periodica Polytechnica Chemical Engineering 2014; 58 (1): 37–46.
44. Sarafraz MM, Hormozi F, Silakhori M. *et al.* On the fouling formation of functionalized and non-functionalized carbon nanotube nano-fluids under pool boiling condition. Applied Thermal Engineering 2016; 95: 433–444.
45. Sarafraz MM. Experimental investigation on pool boiling heat transfer to formic acid, propanol and 2-butanol pure liquids under the atmospheric pressure. Journal of Applied Fluid

Mechanics 2013; 6 (1): 73–79.
46. Nakhjavani M, Nikkhah V, Sarafraz MM *et al*. Green synthesis of silver nanoparticles using green tea leaves: Experimental study on the morphological, rheological and antibacterial behavior. Heat and Mass Transfer 2017; 53 (10): 3201–3209.
47. Sarafraz MM, Nikkhah V, Madani SA, *et al*. Low-frequency vibration for fouling mitigation and intensification of thermal performance of a plate heat exchanger working with CuO/water nanofluid. Applied Thermal Engineering 2017; 121: 388–399.
48. Sarafraz MM, Hormozi F. Application of thermodynamic models to estimating the convective flow boiling heat transfer coefficient of mixtures. Experimental Thermal and Fluid Science 2014; 53: 70–85.
49. Sarafraz MM, Arya A, Nikkhah V. *et al.* Thermal performance and viscosity of biologically produced silver/coconut oil. Nanofluids Chemical and Biochemical Engineering Quarterly 2017; 30 (4): 489–500.